

Received July 16, 2019, accepted July 26, 2019, date of publication August 26, 2019, date of current version September 16, 2019.

Digital Object Identifier 10.1109/ACCESS.2019.2937598

Efficient Algorithm for Scattering by a Large Cluster of Moving Objects

HAI-LI ZHANG¹, YI-XIN SHA², XIAO-YANG HE², XING-YUE GUO²,
AND MING-YAO XIA², (Senior Member, IEEE)

¹School of Electronic Science and Engineering, University of Electronic Science and Technology of China, Chengdu 611731, China

²Department of Electronics, School of Electronics Engineering and Computer Science, Peking University, Beijing 100871, China

Corresponding author: Ming-Yao Xia (myxia@pku.edu.cn)

This work was supported by the NSFC under Project 61531001 and Project 61271032.

ABSTRACT A highly efficient algorithm for analysis of electromagnetic scattering by a large cluster of independently moving objects is proposed in this paper. A double octree structure is introduced, which consists of a main octree stationary to the cluster as a whole, and many sub-octrees moving with individual objects. Based on the new double octree structure, the computation of interactions between two elements is divided into four categories: the two elements are on the same object and are near; the two elements are on the same object but are far; the two elements are on different objects but the two objects are adjacent; the two elements are on different objects and the two objects are non-adjacent. For different interacting categories, different approaches are adopted to maximize the computing efficiency. The new algorithm enables possible fast simulations of scattering by hundreds of independently moving objects. Compared with the conventional Multilevel Fast Multipole Algorithm (MLFMA) and the recently developed Multi-Moving-Object (MMO)-MLFMA, the present scheme has substantial improvement in saving CPU time, providing a viable solution for engineering applications. Numerical validations for accuracy and efficiency are performed.

INDEX TERMS Cluster of moving objects, fast algorithm, scattering analysis.

I. INTRODUCTION

In the past few decades, research on algorithms for analyses of electromagnetic (EM) scattering has achieved a series of brilliant achievements. It plays an important role in many areas, such as microwave remote sensing, radar target recognition and imaging. Accurate and efficient analysis of electrically large and complex structures has always been a hot topic in computational electromagnetics (CEM). Simulations of scattering by a single or a group of moving objects have drawn much attention, as well.

There exist some reports in the literature on analyses of scattering by a single moving object. Scattering by a moving perfectly electrical conducting (PEC) mirror was analyzed using the finite difference time domain (FDTD) method in one and two dimensions [1]. Based on the time domain integral equation (TDIE) method along with the frame hopping method, a numerical approach for the analysis of transient scattering by an accelerated body was presented [2].

The associate editor coordinating the review of this article and approving it for publication was Lei Zhao.

Using relativistic transforms, including space-time transform, EM field transform, and arbitrary reference system transform, scattering by an arbitrary moving object was considered [3]. In [4], a Lorentz finite difference time domain algorithm was proposed to analyze scattering by a moving conducting body.

As for analyses of scattering by multiple motionless objects, extensive researches can be found. To reduce the core memory requirement, a step moment method (SMM) was presented in [5]. In [6], based on the decomposition of strong and weak interactions and fast Fourier transform (FFT) technique, a sparse-matrix canonical-grid (SMCG) method was developed for analyses of scattering by many scatterers. In [7], the characteristic basis function method (CBFM) was used to analyze the scattering by two dimensional multiple PEC elliptical cylinders and square cylinders. In [8], the characteristic modal Green function was introduced for analysis of scattering by multiple bodies of revolution. A domain decomposition method (DDM) for analyses of radiation and scattering from multiple objects can be found in [9]. The DDM method greatly reduces the computational burden of information exchange between

the electrically large sub-regions. An extended equivalence principle algorithm (EPA) was proposed to analyze scattering from multiple bodies of revolution with the axes arbitrarily oriented [10]. In [11], an improved geometric-optics/physical-optics (GO/PO) method was presented to analyze the Terahertz-wave scattering by multiple small-scale grooves. In [12], a simplified model was adopted to characterize the effects of scattering by multiple human bodies that may block the indoor links of the fifth generation (5G) communications.

Previous studies are focused on a single moving object or multiple motionless objects, and there are few studies on a great number of moving objects. The main challenge exists in efficient calculations of couplings between different objects when there are moving independently, i.e., their relative locations and attitudes are changing over time.

Recently, a tailored MMO-MLFMA was presented to meet the need for analyses of scattering by multiple moving objects [13]. A double octree meshing was introduced in the approach. For interactions of two elements that are on the same object and are near, direct integration is used. For interactions of two elements that are on the same object but are not near, the conventional MLFMA [14] is used. For interactions of two elements that are on different objects, the MMO-MLFMA is used. However, as the number of objects is continuously increased, further improvement of the MMO-MLFMA is expected, which is the purpose of the present work. The new algorithm for scattering by a large cluster of moving objects is termed Multi-Level Multiple-Moving-Object MLMFA (ML-MMO-MLFMA) in this work.

II. METHOD

A. DOUBLE OCTREE STRUCTURE

It is supposed that there are a large cluster of objects, the number can be several hundreds, residing in the air, and each object can move and rotate independently. Each object has complex structure and should be meshed with many elements, i.e., they cannot be regarded as point targets. There exist electromagnetic couplings between the objects, which affect the scattering behavior of individual objects, as well as the overall scattering characteristics of the cluster as a whole. Because the location and attitude of each object are changing with time, the scattering properties of the cluster vary over time, too. However, the changes of locations and attitudes are negligible within the duration of a radar pulse, which is typically on the order of microsecond. So the “stop-go-stop” model can be used, i.e., the objects can be taken to be stationary when they are interacting with a radar pulse, and then jump to next locations and attitudes to interact with the next pulse. As a result, the continuous scattering process can be simulated at a series of discrete moments.

In the MMO-MLFMA, interactions between two elements belonging to two different objects need to be recalculated at every moment, while the interactions between every pair of objects are of $O(N^2)$, where N is the number of objects. Reducing the computing complexity from $O(N^2)$ to

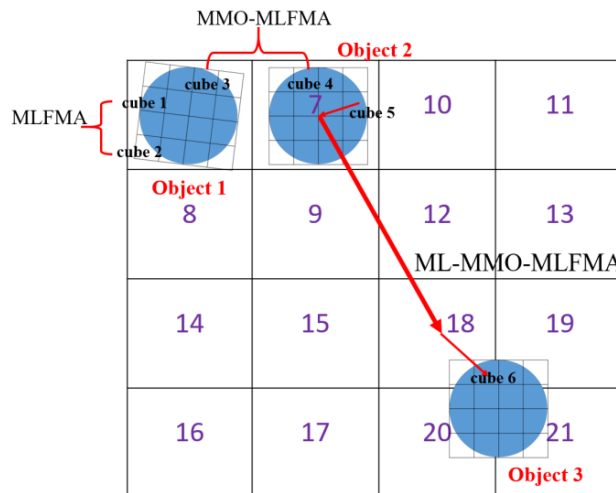


FIGURE 1. Double octree structure for enhanced MMO-MLFMA.

$O(N \ln N)$ is expected as N becomes very large. To this end, a double octree structure is adopted, as shown in Figure 1. For each object, an object-fixed sub-octree is introduced, similar to the conventional MLFMA, i.e., a big cube is used to enclose the object, and then it is successively divided into eight smaller cubes until the size of the smallest cubes is about one quarter wavelength.

In addition to the many sub-octrees, a main octree structure is used to enclose all of the objects. It is stationary, i.e., no object can move out of the domain during the period of simulations. The size of the smallest cubes is about the dimension of one object. So the number of layers of the main octree depends on the total number of objects.

Refer to Figure 1. For calculations of interactions between elements at the same object, say at object 1, an element in cube 1 interacting with an element in cube 2, the conventional MLFMA is applied. For calculations of couplings between two adjacent objects, say object 1 and object 2, the MMO-MLFMA is employed. If the two objects are non-adjacent, say object 2 and object 3, we will adopt an enhanced MMO-MLFMA to calculate their couplings. First, we aggregate the cube information on the highest level of each object to the main octree. Then, transfer the information between cubes in the main octree. Last, disaggregate the information from the main octree to the sub-octrees. This manner is similar to the traditional MLFMA if each object is seen as a ‘macro-element,’ so that the computing complexity of couplings between the objects is reduced from $O(N^2)$ by using MMO-MLFMA to $O(N \ln N)$ by using ML-MMO-MLFMA, as illustrated in Figure 2.

B. FORMULATIONS

After discretization, we would finally obtain a matrix equation for the problem at the moment t_n , which takes the form of

$$\{b(t_n)\} \triangleq [Z(t_n)] \{a(t_n)\} = \{e(t_n)\} \tag{1}$$

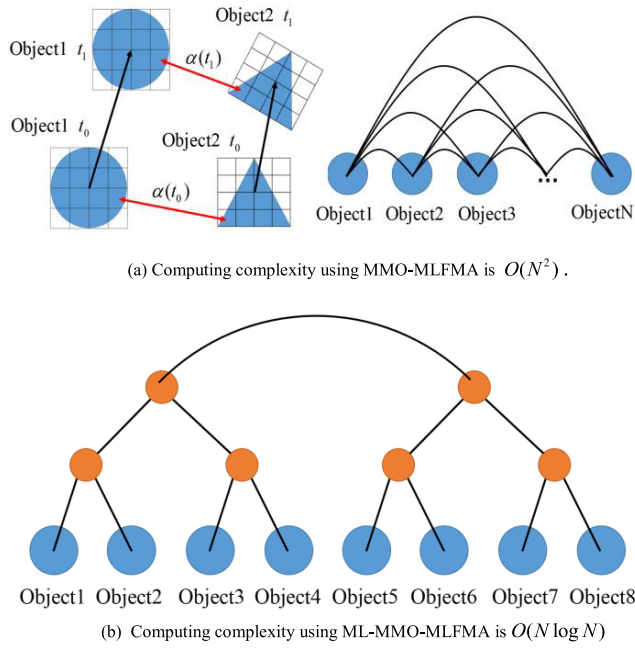


FIGURE 2. Computing complexities by MMO-MLFMA and ML-MMO-MLFMA.

where $\{e(t_n)\}$ represents the excitation vector, $\{b(t_n)\}$ defines the scattering contribution from all of the source elements $\{a(t_n)\}$. Let $b_{q,j}(t_n)$ be an entry of $\{b(t_n)\}$, which accounts for the total scattering contribution at the j -th element on the q -object by all source elements.

Suppose that the j -th element is situated in the m -th cube on the q -th object. According to the grouping relation, the source elements can be divided into four categories:

- (i) On the q -th object and in the m -th cube or in those cubes near to the m -th cube. The interactions will be calculated directly using numerical integrations.
- (ii) On the q -th object but in those cubes not near to the m -th cube. The interactions will be calculated by the conventional MLFMA.
- (iii) On those objects adjacent to the q -th object. The interactions will be calculated by the MMO-MLFMA.
- (iv) On those objects not adjacent to the q -th object. The interactions will be calculated by the ML-MMO-MLFMA to be described below.

Therefore, we can write $b_{q,j}(t_n)$ as:

$$\begin{aligned}
 b_{q,j}(t_n) &= \sum_{p=1}^{N_{\text{Object}}} \sum_{i=1}^{N_q} Z_{q,j;p,i}(t_n) a_{p,i}(t_n) \\
 &= \sum_{i=1}^{N_{q,\text{Near}}} Z_{q,j;q,i}^{\text{Near}}(t_n) a_{q,i}(t_n) + \sum_{i=1}^{N_{q,\text{Far}}} Z_{q,j;q,i}^{\text{Far}}(t_n) a_{q,i}(t_n) \\
 &\quad + \sum_{p1=1}^{N_{\text{Near, Object}}} \sum_{i=1}^{N_{p1}} Z_{q,j;p1,i}^{\text{Near}}(t_n) a_{p1,i}(t_n) \\
 &\quad + \sum_{p2=1}^{N_{\text{Far, Object}}} \sum_{i=1}^{N_{p2}} Z_{q,j;p2,i}^{\text{Far}}(t_n) a_{p2,i}(t_n). \tag{2}
 \end{aligned}$$

The four terms are corresponding to the four categories above. The **first** term does not need further explanation. For the **second** term to be calculated by the MLFMA, the matrix element can be written in the form of

$$\begin{aligned}
 Z_{q,j;q,i}^{\text{Far}} &= \left[V_{fjm}^q \right] \cdot (\bar{\beta}_{l_1 l_2}^q \cdots \bar{\beta}_{l_{L-1} l_L}^q) \cdot \bar{T}_{l_L, l'_L}^{qq} \\
 &\quad \cdot (\bar{\beta}_{l'_L l'_{L-1}}^q \cdots \bar{\beta}_{l'_2 l'_1}^q) \cdot \left[V_{sm'i}^q \right] \tag{3}
 \end{aligned}$$

with

$$V_{fjm}^q(\hat{k}, t_n) = \int_S dS e^{-j\mathbf{k} \cdot [\mathfrak{R}^q(t_n) \mathbf{r}_{jm}]} [\bar{\mathbf{I}} - \hat{k}\hat{k}] \cdot [\mathfrak{R}^q(t_n) \cdot \mathbf{t}_j^q(\mathbf{r}_{jm})] \tag{4}$$

$$V_{sm'i}^q(\hat{k}, t_n) = \int_S dS' e^{-j\mathbf{k} \cdot [\mathfrak{R}^q(t_n) \mathbf{r}_{im'}]} [\bar{\mathbf{I}} - \hat{k}\hat{k}] \cdot [\mathfrak{R}^q(t_n) \cdot \mathbf{j}_i^q(\mathbf{r}_{im'})] \tag{5}$$

$$\begin{aligned}
 \bar{T}_{l_L, l'_L}^{qq}(\hat{r}_{mm'} \cdot \hat{k}) &= \sum_{i=0}^L (-j)^i (2l+1) h_l^{(2)}(kr_{mm'}) P_l(\hat{r}_{mm'} \cdot \hat{k}) \tag{6}
 \end{aligned}$$

in which $\mathfrak{R}^q(t_n)$ stands for the coordinate system transform. At moment t_n , $\mathfrak{R}^q(t_n)$ can transform the q -th object-fixed coordinate system to the global coordinate system. $[V_{sm'i}^q]$ is responsible for the information transmission from the point i to the center of the m' -th cube in the q -th object. $[V_{fjm}^q]$ disseminates the information from the center of the m -th cube to point j in the q -th object. Matrix \bar{T}_{l_L, l'_L}^{qq} is used for information transmission between all elements residing in the two cubes in the q -th object, which is a diagonal matrix. The parts $(\bar{\beta}_{l'_L l'_{L-1}}^q \cdots \bar{\beta}_{l'_2 l'_1}^q)$ and $(\bar{\beta}_{l_1 l_2}^q \cdots \bar{\beta}_{l_{L-1} l_L}^q)$ are responsible for aggregation and disaggregation, respectively. For detailed expressions of these symbols, please refer to [15]. For the **third** term to be calculated by MMO-MLFMA, the impedance matrix element is written as:

$$\begin{aligned}
 Z_{q,j;p1,i}^{\text{Near}} &= \left[V_{fjm}^q \right] \cdot (\bar{\beta}_{l_1 l_2}^q \cdots \bar{\beta}_{l_{L-1} l_L}^q) \cdot \bar{T}_{l_L, l'_L}^{qp1} \\
 &\quad \cdot (\bar{\beta}_{l'_L l'_{L-1}}^{p1} \cdots \bar{\beta}_{l'_2 l'_1}^{p1}) \cdot \left[V_{sm'i}^{p1} \right]. \tag{7}
 \end{aligned}$$

Matrix $\bar{T}_{l_L, l'_L}^{qp1}$, which is also a diagonal matrix, is used for information transmission between all elements residing in the pair of cubes, which belong to the q -th object and the p -th object, respectively. For the **fourth** term, the interaction between those elements on different objects which are non-adjacent can be expressed by

$$\begin{aligned}
 Z_{q,j;p2,i}^{\text{Far}} &= \left[V_{fjm}^q \right] \cdot (\bar{\beta}_{l_1 l_2}^q \cdots \bar{\beta}_{l_{L-1} l_L}^q) \\
 &\quad \cdot (\bar{\gamma}_{l_1 l_2} \cdots \bar{\gamma}_{l_{L-1} l_L} \cdot \bar{T}_{l_L, l'_L} \cdot \bar{\gamma}_{l'_L l'_{L-1}} \cdots \bar{\gamma}_{l'_2 l'_1}) \\
 &\quad \cdot (\bar{\beta}_{l'_L l'_{L-1}}^{p2} \cdots \bar{\beta}_{l'_2 l'_1}^{p2}) \cdot \left[V_{sm'i}^{p2} \right] \tag{8}
 \end{aligned}$$

where $\bar{\gamma}_{l_1 l_2}, \dots, \bar{\gamma}_{l_{L-1} l_L}$ are responsible for the information transmission from the sub-octrees on each sub-object to the main octree, and the aggregation process in the main octree. $\bar{\gamma}_{l'_L l'_{L-1}} \cdots \bar{\gamma}_{l'_2 l'_1}$ are responsible for the disaggregation process

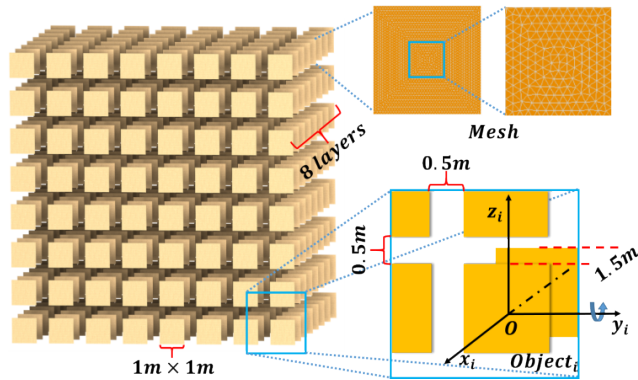


FIGURE 3. A square metal plate array. Each plate is rotatable about its y -axis.

in the main octree, and the information transmission from the main octree to the sub-octrees on each object. Matrix \bar{T}_{L_i, L_i} conducts the information transmission between two objects efficiently. By the way, it should be noticed that the part $\left(\left[V_{f_{mj}}^q \right] \cdot \bar{\beta}_{l_1 l_2}^q \cdots \bar{\beta}_{l_{L-1} l_L}^q \right)$ in (3), (7) and (8) are the same, which needs to be calculated just once to further reduce the computing load.

C. SAI PRECONDITION

Sparse approximate inverse (SAI) is a valuable scheme to precondition a matrix equation for convergence acceleration [16]. It is noticed that $Z_{q,j;q,i}^{Near}(t_n)$ in the first term of (2) is actually independent of moment t_n , because it accounts for the near interactions between elements on the same objects. Therefore, the near interacting matrix is taken the form of diagonal blocks:

$$\left[Z^{Near} \right] \approx \begin{bmatrix} Z_{1;1}^{Near} & & & \\ & Z_{2;2}^{Near} & & \\ & & \ddots & \\ & & & Z_{N_{Object};N_{Object}}^{Near} \end{bmatrix} \quad (9)$$

where $Z_{q;q}^{Near}$ ($q = 1, \dots, N_{Object}$) represents the near interactions of elements residing on the q -th object. The approximate inverse of (9) is easy to solve, and is denoted as $\left[Z^{Near} \right]^{-1} \approx [P]$, which is unchanged with the time. Multiplying (1) by $[P]$, we obtain the final preconditioned equation.

III. NUMERICAL RESULTS

All simulations are conducted on a PC with a Intel i-6700K CPU of 4.0 GHz and core memory of 32 GB, using linux operating system. The biconjugate gradient stabilized method (BICGSTAB) is used to solve the linear equations. The RWG basis functions are used to discretize the integral equations with Galerkin method.

The first example is a scattering problem by an array consisting of 512 rotatable square metal plates. They are arranged as a $8 \times 8 \times 8$ array as shown in Figure 3. Each plate is able to rotate about an axis. The side length is 1 m.

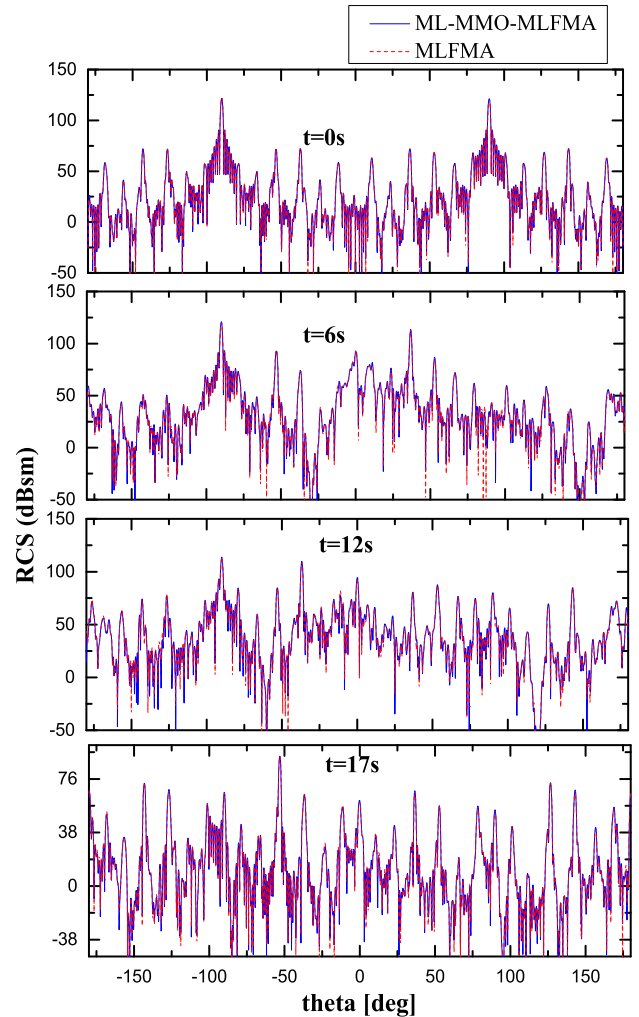


FIGURE 4. Bi-static RCS of the rotating metal plate array at four moments.

Each plate is modeled by 2,204 small triangular patches, which results in 3,240 unknowns. Thus the total number of unknowns is 1,658,880. The metal plates are open objects, so that the electric field integral equation (EFIE) is adopted for this example.

Suppose that each plate is rotating about its local y -axis at an angular speed of 5 Degrees/s. The incident wave is a plane wave at 1 GHz. The incident direction is along the global x -axis, and the electric field is z -axis polarized.

Figure 4 shows the results of bi-static radar cross-section (RCS) in the xz -plane at four time points. The results obtained by using the ML-MMO-MLFMA and the traditional MLFMA are found in good agreements, which demonstrate the correctness and accuracy of the proposed ML-MMO-MLFMA. Figure 5 show the backscattering RCS of the rotational array at 17 moments.

The second example is a large cluster consisting of 42 moving cone-like objects. The geometry of a single object is shown in Figure 6 (a) and (b), with a height of 0.6 m and a base diameter of 0.4 m. As shown in Figure 6 (c),

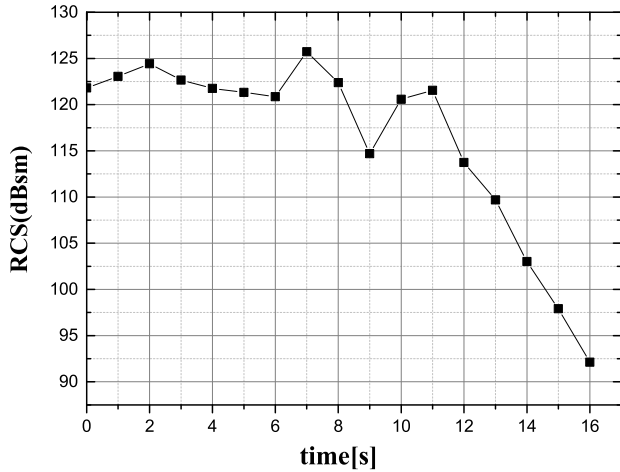


FIGURE 5. Backscattering RCS of the rotating metal plate array at 17 moments.

TABLE 1. Velocity and position parameters of the seven groups.

<i>i</i>	1	2	3	4	5	6	7
v_x	20	-20	-40	-20	20	40	0
v_y	300	300	300	300	300	300	300
v_z	-45.36	-45.36	-80	-114.64	-114.64	-80	-80
x_0	0.5	-0.5	-1.0	-0.5	0.5	1.0	0
y_0	0	0	0	0	0	0	0
z_0	0.866	0.866	0	-0.866	-0.866	0	0

each object is meshed with 2,690 triangular patches, which results in 4,035 unknowns using the RWG basis functions. So the total number of unknowns is 169,470. The cluster is divided into seven groups, each of which has six objects. The coordinates of the j -th ($j = 1, 2, \dots, 6$) object in the i -th ($i = 1, 2, \dots, 7$) group are given by

$$\begin{cases} x_{i,j}(t) = x_0^i + v_x^i(t + t_0^j) \\ y_{i,j}(t) = y_0^i + v_y^i(t + t_0^j) \\ z_{i,j}(t) = z_0^i + v_z^i(t + t_0^j) \end{cases} \quad (10)$$

The values of $x_0^i, v_x^i, y_0^i, v_y^i, z_0^i, v_z^i$ are list in detail in Table I and $t_0^j = 0.005(j - 1)$ is used. As shown in Figure 6 (d), each object is supposed to rotate around its x -axis at -1000 Degrees/s. Because the cone-like objects are close bodies, the combined field integral equation (CFIE) has been adopted for this example.

A plane wave at 1 GHz is incident upon the cluster along the x -axis direction, i.e., by means of side-looking. The electric field is z -polarized. The bi-static RCS in the xz -plane at four moments are shown in Figure 7. The results by the present ML-MMO-MLFMA and the conventional MLFMA are consistent. Some comparisons for computing efficiencies of the present ML-MMO-MLFMA with the

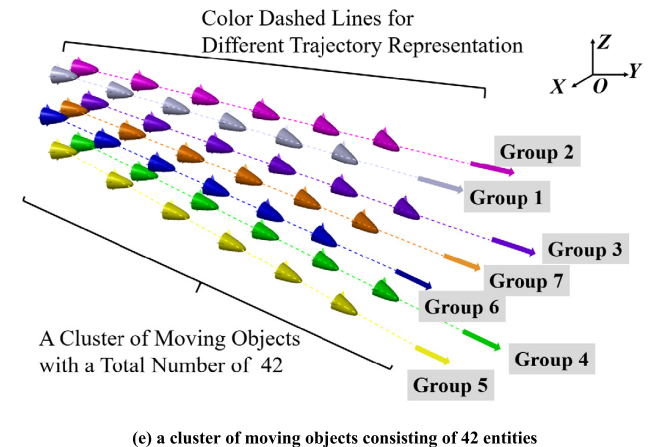
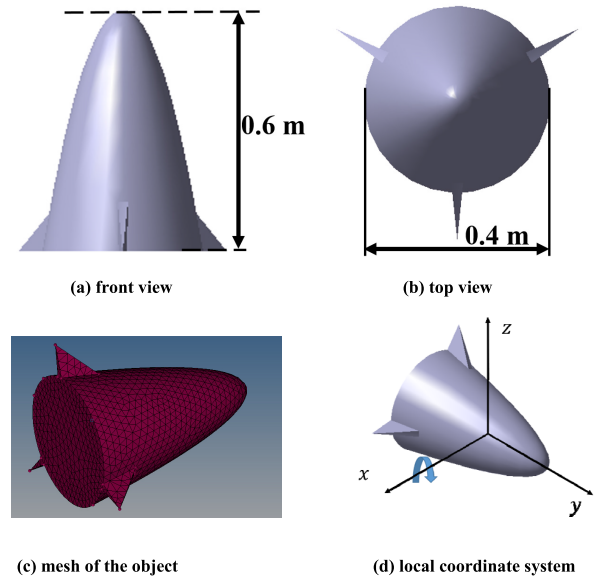


FIGURE 6. Geometry of one object and a cluster comprising of seven groups, each with six objects.

traditional MLFMA and the previous MMO-MLFMA are given in Table II.

From the table, we can see that: by using the traditional MLFMA, it would take $228.47 * 200 = 45,694$ s or 12.7 hrs for simulation at 200 moments; by using the MLFMA with SAI, it would take $169.05 + (354.18 - 169.05) * 200 = 37,195$ s or 10.3 hrs for 200 moments if the SAI needs computing only once; by using the MMO-MLFMA, it takes 29,165 s or 8.1 hrs for 200 moments; by using the present ML-MMO-MLFMA, it takes 22,212 s or 6.2 hrs for 200 moments, which is about the half of that by the traditional MLFMA. Therefore, the saving of CPU time is appreciable for continuously simulating at many moments within a time frame for radar tracking of a cluster of objects. Please note that the SAI matrix in the MLFMA is full-sized of dimension N by N ($N = 169,740$ in this example), and the solving time is 169.05 s. However, in the ML-MMO-MLFMA, the near interacting matrix takes the form of (9) and all the

TABLE 2. Performance comparisons of MLFMA, MMO-MLFMA and ML-MMO-MLFMA.

	MLFMA (at $t=0.01s$)	MLFMA (at $t=0.01s$ with SAI)	MMO-MLFMA		ML-MMO-MLFMA	
			Average	200 moments	Average	200 moments
Time of filling matrix (s)	126.04	126.04	100.4	20080	55.65	11130
Time of SAI matrix (s)	0.0	169.05	0.0217	4.34	0.0217	4.34
Number of iterations	22	9	5.42	1084	5.42	1084
Time of solving equation (s)	100.15	47.77	40.255	8051	55.38	11076
Total CPU time (s)	228.47	354.18	145.83	29165	111.06	22212
Memory requirement (MB)	599	827	24640		1244	

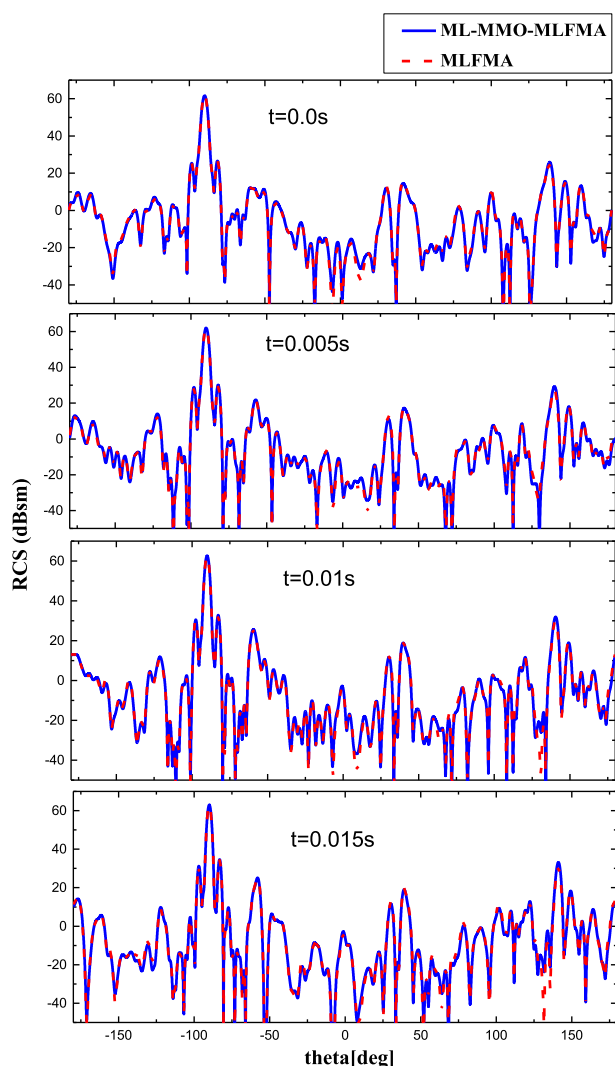


FIGURE 7. Bi-static RCS in xz -plane of the moving cluster of objects shown in Fig. 6 (e) at four moments.

sub-matrices are identical in this example, so we just need to solve the SAI for one sub-matrix, and it takes only 4.34 s. In the last row of Table II, the memory requirements by using the different schemes are given. The MMO-MLFMA

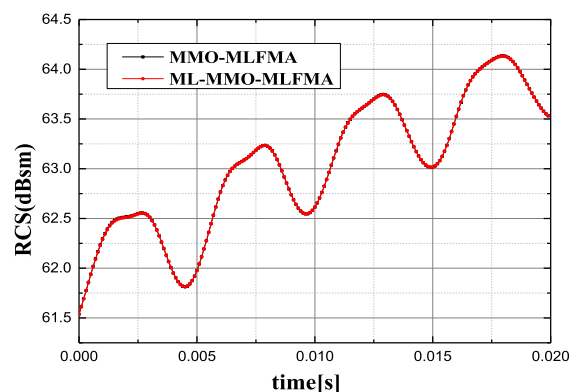


FIGURE 8. Backscattering RCS of the moving object cluster shown in Fig. 6 (e) at 200 moments.

occupies too much memory because it needs to store the transmission matrices between the top levels of every two objects. This results in a radical increase of memory occupation by a factor of about the number of objects (=42 in this example), though it may be mitigated through optimizing the codes. The memory requirement of ML-MMO-MLFMA is about two times of that of the traditional MLFMA, and much less than that of the MMO-MLFMA, which is one reason that we upgrade the previous MMO-MLFMA to the present ML-MMO-MLFMA.

Figure 8 shows the simulation results at 200 moments at a time step of 0.0001 s, and the total lasting time is 0.02 s. In the whole process, the results of the ML-MMO-MLFMA and the MMO-MLFMA are consistent. During this 0.02 s, the objects have rotated 20 degrees, and a quasi-periodic oscillating of the backscattering RCS is observed. It is also observed that the RCS tends to increase with the time. This reflects the fact that the cluster of objects tends to diverge, which makes it look larger and larger.

IV. CONCLUSION

In this paper, a significant extension of the previous MMO-MLFMA, termed ML-MMO-MLFMA, suiting for simulation of scattering by a large cluster of independently moving objects, is developed. It lies on a double octree

grouping scheme, i.e., a stationary main octree that encloses all the objects with the smallest cube about the dimension of a single object, and many object-fixed sub-octrees that are moving with individual objects. It calculates the interactions between two elements in four ways. For two elements that reside on the same object and are near in the sub-octree, direct numerical integration is used. This part of interacting matrix is unchanged with time and is used for preconditioning. For two elements that reside on the same object but are not near in the sub-octree, the conventional MLFMA is used. For two elements that reside on two different objects but the two objects are adjacent in the main octree, the MMO-MLFMA is used. Finally, for two elements that reside on two different objects and the two objects are not adjacent, the ML-MMO-MLFMA is used. The proposed approach is particularly valuable for engineering applications involved in continuous simulations such as radar tracking of a large cluster of objects, which even permits each object to move or/and to rotate independently.

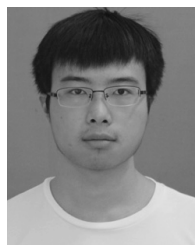
REFERENCES

- [1] F. Harfoush, A. Taflove, and G. A. Kriegsmann, "A numerical technique for analyzing electromagnetic wave scattering from moving surfaces in one and two dimensions," *IEEE Trans. Antennas Propag.*, vol. 37, no. 1, pp. 55–63, Jan. 1989.
- [2] S. Q. Jia, X. M. Jiang, and M. Y. Xia, "Numerical approach for analysis of transient scattering by an accelerated body," *J. Electromagn. Waves Appl.*, vol. 26, nos. 4–5, pp. 770–782, 2012.
- [3] S. Q. Jia and M. Y. Xia, "Numerical simulation of electromagnetic scattering by moving objects based on relativity," *Acta Scientiarum Naturalium Univ. Pekinensis*, vol. 49, no. 6, pp. 1111–1117, Nov. 2013.
- [4] K.-S. Zheng, J.-Z. Li, G. Wei, and J.-D. Xu, "Analysis of Doppler effect of moving conducting surfaces with Lorentz-FDTD method," *J. Electromagn. Waves Appl.*, vol. 27, no. 2, pp. 149–159, Nov. 2012.
- [5] Y. Xu, H. Yang, R. Shen, L. Zhu, and X. Huang, "Scattering analysis of multiobject electromagnetic systems using stepwise method of moment," *IEEE Trans. Antennas Propag.*, vol. 67, no. 3, pp. 1740–1747, Mar. 2019.
- [6] C. H. Chan and L. Tsang, "A sparse-matrix canonical-grid method for scattering by many scatterers," *Microw. Opt. Technol. Lett.*, vol. 8, no. 2, pp. 114–118, Feb. 1995.
- [7] Y. F. Sun, Y. Zhang, S. J. Xu, and X. Q. Chen, "EM scattering analysis of 2-D multiple conducting cylinders using characteristic basis function method," *Chin. J. Radio Sci.*, vol. 21, no. 2, pp. 229–232, Feb. 2006.
- [8] J. Hu, Y.-K. Li, Z. Nie, and H. Zhao, "Modal characteristic basis function method for solving scattering from multiple conducting bodies of revolution," *IEEE Trans. Antennas Propag.*, vol. 62, no. 2, pp. 870–877, Feb. 2014.
- [9] K. Zhao, V. Rawat, and J. F. Lee, "A domain decomposition method for electromagnetic radiation and scattering analysis of multi-target problems," *IEEE Trans. Antennas Propag.*, vol. 56, no. 8, pp. 2211–2221, Aug. 2008.
- [10] T. Su, L. Du, and R. Chen, "Electromagnetic scattering for multiple PEC bodies of revolution using equivalence principle algorithm," *IEEE Trans. Antennas Propag.*, vol. 62, no. 5, pp. 2736–2744, May 2014.
- [11] X. Meng, L. X. Guo, C. L. Dong, and Y. C. Jiao, "GO/PO method for the terahertz scattering computation of objects with multiple small-scale grooves," *IEEE Access*, vol. 7, pp. 40738–40745, 2019.
- [12] Y. Dalveren, A. H. Alabish, and A. Kara, "A simplified model for characterizing the effects of scattering objects and human body blocking indoor links at 28 GHz," *IEEE Access*, vol. 7, pp. 69687–69691, 2019.
- [13] H. L. Zhang, Y. X. Sha, X. Y. Guo, M. Y. Xia, and C. H. Chan, "Efficient analysis of scattering by multiple moving objects using a tailored MLFMA," *IEEE Trans. Antennas Propag.*, vol. 67, no. 3, pp. 2023–2027, Mar. 2019.
- [14] C.-C. Lu and W. C. Chew, "A multilevel algorithm for solving a boundary integral equation of wave scattering," *Microw. Opt. Technol. Lett.*, vol. 7, no. 10, pp. 466–470, Jul. 1994.
- [15] W. C. Chew, J. M. Jin, E. Michielssen, and J. Song, *Fast and Efficient Algorithms in Computational Electromagnetics*. Boston, MA, USA: Artech House, 2001.
- [16] J. Lee, J. Zhang, and C.-C. Lu, "Sparse inverse preconditioning of multilevel fast multipole algorithm for hybrid integral equations in electromagnetics," *IEEE Trans. Antennas Propag.*, vol. 52, no. 9, pp. 2277–2287, Sep. 2004.

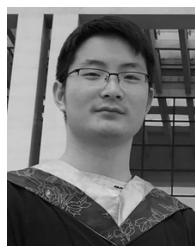


HAI-LI ZHANG received the B.S. degree in physics from Anhui Normal University, Wuhu, China, in 2014. He is currently pursuing the Ph.D. degree with the University of Electronic Science and Technology of China, Chengdu. From June 2016 to September 2016, he was a Research Assistant with the Department of Electronic Engineering and the State Key Laboratory of Millimeter Waves, City University of Hong Kong, Hong Kong. Since October 2017, he has been an

Exchange Student with the School of Electronics Engineering and Computer Science, Peking University, Beijing, China. His research interest includes computational electromagnetics with fast algorithm.



YI-XIN SHA received the B.E. degree in electronic information engineering from Anhui University, Hefei, China, in 2017. He is currently pursuing the Ph.D. degree with the School of Electronics Engineering and Computer Science, Peking University, Beijing, China. His research interests include computational electromagnetics and multi-physics modeling.



XIAO-YANG HE received the B.S. degree in physics from Lanzhou University, Lanzhou, China, in 2017. He is currently pursuing the Ph.D. degree with the School of Electronics Engineering and Computer Science, Peking University, Beijing, China. His current research interests include computational electromagnetics and machine learning.



Her research interests include computational electromagnetics and applications.

XING-YUE GUO received the B.S. degree in electronic information science and technology from Southwest Jiaotong University, Chengdu, China, in 2011, and the M.E. degree from the University of Electronic Science and Technology of China, Chengdu, in 2014. She is currently pursuing the Ph.D. degree with the School of Electronics Engineering and Computer Science, Peking University, Beijing, China. From 2014 to 2017, she was a Research Assistant with the CAEP Software Center for High Performance Numerical Simulation, Beijing.



Assistant and a Research Fellow, respectively, with the City University of Hong Kong. He joined Peking University as an Associate Professor, in 2002, and was promoted to a Full Professor, in 2004. He moved to the University of Electronic Science and Technology of China as a Chang-Jiang Professor nominated by the Ministry of Education of China, in 2010. He returned to Peking University after finishing the appointment, in 2013. His research interests include electromagnetic theory, numerical methods and applications, such as wave propagation and scattering, electromagnetic imaging and probing, microwave remote sensing, antennas, and microwave components. He was a recipient of the Young Scientist Award of the URSI, in 1993, the First-Class Prize on the Natural Science by the Chinese Academy of Sciences, in 2001, and the Foundation for Outstanding Young Investigators presented by the National Natural Science Foundation of China, in 2008. He served as an Associate Editor for the IEEE TRANSACTIONS ON ANTENNAS AND PROPAGATION.

• • •